International Journal of Electrical, Electronic and Communication Sciences
ISSN: 2517-9438
Vol:11, No:2, 2017

An Efficient Tool for Mitigating Voltage Unbalance with Reactive Power Control of Distributed Grid-Connected Photovoltaic Systems

Malinwo Estone Ayikpa

***Abstract*—**With the rapid increase of grid-connected PV systems over the last decades, genuine challenges have arisen for engineers and professionals of energy field in the planning and operation of existing distribution networks with the integration of new generation sources. However, the conventional distribution network, in its design was not expected to receive other generation outside the main power supply. The tools generally used to analyze the networks become inefficient and cannot take into account all the constraints related to the operation of grid-connected PV systems. Some of these constraints are voltage control difficulty, reverse power flow, and especially voltage unbalance which could be due to the poor distribution of single-phase PV systems in the network. In order to analyze the impact of the connection of small and large number of PV systems to the distribution networks, this paper presents an efficient optimization tool that minimizes voltage unbalance in three-phase distribution networks with active and reactive power injections from the allocation of single-phase and three-phase PV plants. Reactive power can be generated or absorbed using the available capacity and the adjustable power factor of the inverter. Good reduction of voltage unbalance can be achieved by reactive power control of the PV systems. The presented tool is based on the three-phase current injection method and the PV systems are modeled via an equivalent circuit. The primal-dual interior point method is used to obtain the optimal operating points for the systems.

***Keywords*—**Photovoltaic generation, primal-dual interior point method, three-phase optimal power flow, unbalanced system.

I. Introduction

POWER quality studies for the electric power systems have always been done with conventional methods based on allocation of capacitor [1], [2], reactive power and voltage control [3], [4], voltage stability [5], taps adjustment of OLTCs and voltage regulator [6], [7], state estimation [8], [9]. However, in the last decade much effort has been concentrated on the integration of distributed generation (DG) sources in the distribution networks. Some studies present the impact of DG on electric power systems, [10], [11], other, the planning and management policy of the distribution and transmission systems with DG [12], [13]. Among the DG sources, photovoltaic (PV) is part of those with greatest growth. The integration of PV systems in distribution networks may cause positive as well as negative impacts in the planning and operation of these networks. When the optimal placement and size are well defined, grid-connected PV systems can reduce the losses, improve the voltage profile, reduce voltage unbalance, and increase system reliability [11], [14], [15]. Despite its numerous advantages overloaded by the grid-connected PV system, it appears that a large scale of PV systems connected in distribution system can generate several negative impacts. Some of this impacts presented in [16], [17], are related to reverse power flow, voltage increase, power losses, voltage unbalance and an increase of reactive power. The analysis of these impacts on distribution network is not an easy task. In most applications of grid-connected PV systems, the inverters are used only as active power source, thus operating with unit power factor [18]. However, it should be noted that during the hours of maximum generation with high penetration level of PV systems operating with unit power factor, overvoltage problem might occur along distribution feeders [15]. This situation has been a subject of recent researches in which distribution static compensator (DSTATCOM) is used to keep voltages within acceptable limit when PV systems operate during a peak solar irradiation with a high level penetration [19], [20]. With the development of voltage source inverter technology, overvoltage can be limited by voltage regulation function of the inverter, which can operate as reactive power compensator [15], [21]. Researches developed in the last years were principally focused on the reactive power generated by single-phase PV systems [22], [23]. In this paper, single-phase and three-phase PV systems were associated to provide reactive power on the grid. This consideration helps not only to control the size of the PVs installation but also to improve the power quality Tools based only on the single-phase equivalent model may not produce the best operating solutions for three-phase systems, especially when circuits and/or loads are considerably unbalanced [24]. For these reasons, this work models the PV power plants in the three-phase optimal power flow (TOPF) from the PV module equivalent circuit and, with the TOPF, analyzes the impact of the PV generation on the voltage unbalance of distribution systems.

The three-phase representation of the distribution system was first made in power flow programs that use the backward/ forward sweeping method to obtain system voltage [25]. However, in [26] a three-phase current injection method (TCIM) was proposed resulting in better convergence properties than the conventional method. The same formulation was used later in [27].

Several papers on the TOPF problem have been published in recent years. Among them can be cited [28] which proposes

M. E. Ayikpa is with GSP/LABSPOT, Department of Electrical Engineering, Federal University of Santa Catarina (UFSC), 88040-900 – Florianópolis - SC, Brazil (e-mail: lemair2035@gmail.com).

a solution for an unbalanced optimal power flow (OPF) via the Quasi-Newton method; [6] which considers discrete control operations such as capacitor switching and taps adjustment of OLTCs; [29], based on semidefinite programming; [30] which extends the TOPF based on current injections for optimization of n-conductors systems; [7] which achieves optimal adjustment of capacitor banks and voltage regulators to minimize losses and [31], based on locational marginal price concept applied to distribution systems. Some papers also present studies on the impact of distributed PV generation [14], [27], [32].

In this study, PV modules are represented by the five-parameter model [33], [34]. This representation was used in the power flow problem [35] and, more recently, in the single-phase OPF [36] and TOPF problems [37]. This work describes a TOPF model based on the proposed formulation in [27], in which the PV systems are represented by the five-parameter model. Single-Phase and Three-Phase PVs are connected in the distribution networks, providing active and reactive power.

The next section explains how the PV generation is calculated. Section III presents a formulation of the problem with PV systems. Section IV analyzes the results obtained and, finally, Section V summarizes the main conclusions of the study.

II. PV Generation Calculation

A. The Five-Parameter Model

The electrical power supplied by a PV module can be obtained from the equivalent electrical circuit of Fig. 1 [33].

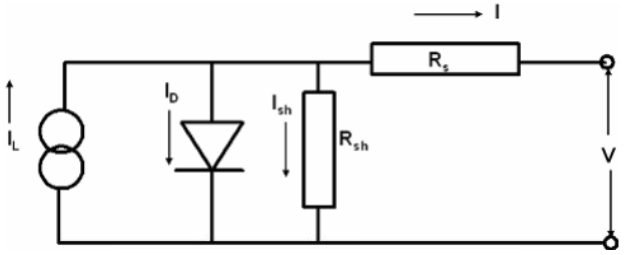

Fig. 1 Equivalent electrical circuit for PV module

Applying Kirchhoff's 1st Law to the circuit, the current injected by the module is:

$$I = I_L - I_o\left[\exp\left(\frac{V + I R_s}{V_t\,\hat{a}}\right) - 1\right] - \frac{V + I R_s}{R_{sh}} \tag{1}$$

where I is the injected current, V the terminal voltage, I_L is the current generated by the incident light, I_0 is the saturation current of the diode, $V_t = N_s k_b T_c/q$ is the thermal voltage of the array with N_s cells connected in series, k_b is the Boltzmann constant, T_c is the temperature (K), q is the electron charge and $\hat{a}$ is the diode ideality constant. When one has the cells array, R_s and R_{sh} are the equivalent resistances.

Once the five parameters, I_L, I_0, R_s, R_{sh} and $\hat{a}$, are known, the current, voltage and active power supplied by the module can be calculated in each scenario of temperature and solar irradiation. However, not all parameters are available, since manufacturers' datasheet of PV modules only provide the nominal open-circuit voltage, $V_{oc,n}$, the nominal short-circuit current, $I_{sc,n}$, voltage and current at the maximum power point, V_{mp} and I_{mp}, the coefficients of temperature for open circuit voltage and short-circuit current, K_V and K_I, and the maximum power produced experimentally, $P_{max,e}$. The values are referred to STC conditions (standard test conditions). Some manufacturers also provide I-V curves for different levels of irradiation and temperature. In [34] an iterative method is proposed to obtain the parameters of equivalent circuit from the information provided by the manufacturers. This method is used to calculate PV generation.

B. Five-Parameter and DC Power Calculation

The method is based on the fact that I_L varies with the temperature and the solar irradiation incident on the PV module according to:

$$I_{L,n} = \left(I_{L,n} + K_I \Delta T\right)\frac{G}{G_n} \tag{2}$$

where $I_{L,n}$ is the current generated at nominal conditions, G the irradiation on the surface of the array, G_n the nominal irradiation and $\Delta T = T - T_n$, where T is the measured temperature and T_n the temperature at nominal conditions.

The saturation current of the diode is obtained in order to match the open circuit voltage with experimental data obtained for different temperatures. The starting point is the nominal saturation current

$$I_{o,n} = I_{sc,n} \Big/ \left[\exp\left(\frac{V_{oc,n}}{V_{t,n}\hat{a}}\right) - 1\right] \tag{3}$$

calculated on the thermal voltage, $V_{t,n}$, of the N_s cells connected in series at the temperature T_n.

I_0 is obtained from (4) employing the voltage and current coefficients K_V and K_I and the temperature correction factor ΔT:

$$I_o = \frac{I_{sc,n} + K_I \Delta T}{\exp\left(\dfrac{V_{oc,n} + K_V \Delta T}{V_{t,n}\hat{a}}\right) - 1} \tag{4}$$

$\hat{a}$ is determined according to the type of technology used in the solar panel, and $\hat{a} = 1{,}3$ for the module used (Hanwha polycrystalline) [38]. R_s and R_{sh} are calculated from the assumption that only a pair $\{R_s, R_{sh}\}$ leads to the maximum power experimentally measured, $P_{\max,e} = V_{mp} I_{mp}$, in the conditions provided by the manufacturer. From (1), it follows that R_s and R_{sh} must respect:

$$P_{\max,e} = V_{mp}\left\{I_L - I_o\left[\exp\left(\frac{V_{mp}+R_s I_{mp}}{V_t \hat{a}}\right)-1\right]-\frac{V_{mp}+R_s I_{mp}}{R_{sh}}\right\} \quad (5)$$

To solve (5), R_s is incremented from zero. R_{sh} is initialized to the minimum value obtained by the inclination of the straight line segment joining the points on the I-V curve defined by the short-circuit and maximum power condition:

$$R_{sh,\min} = \frac{V_{mp}}{I_{sc,n} - I_{mp}} - \frac{V_{oc,n} - V_{mp}}{I_{mp}} \quad (6)$$

For each pair $\{R_s, R_{sh}\}$ the value of I_L is updated using the relation between the currents of the circuit:

$$I_{L,n} = \frac{R_s + R_{sh}}{R_s} I_{sc,n} \quad (7)$$

Fig. 2 shows how R_s and R_{sh} are obtained.

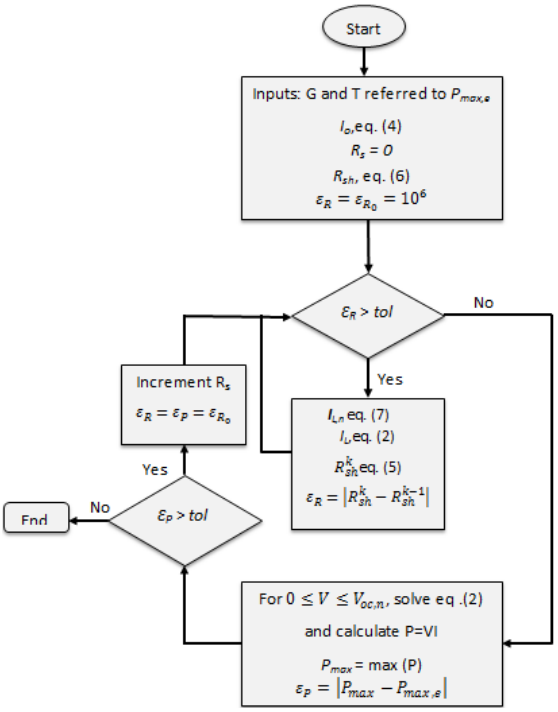

Fig. 2 Algorithm to determine R_s, and R_{sh}

Having found R_s and R_{sh}, I_L, I_0 and the DC power generated P_ω can be calculated for each scenario of temperature and solar irradiation, according to [37].

C. Inverter Modeling and AC Power Calculation

The PV modules are connected in series forming *strings* and these are connected in parallel to the inverters. The number of modules per *string*, $N_{PV,S}$, and the number of *strings*, N_{str}, are chosen in order to achieve a good efficiency of DC-AC conversion. The inverter efficiency was calculated by means of exponential interpolation of the data indicated in the manufacturer's datasheet for each voltage curve, with determination coefficient $R^2 = 0{,}99$. The active AC power at the inverter output is:

$$P_{PV,inv,\omega} = \eta_{inv,\omega} N_{PV,s} N_{str} P_\omega \quad (8)$$

where the efficiency of the inverter is obtained by the function that interpolates the data of the manufacturer ($\eta_{inv,\omega} = f_V(V_{mp,\omega}, I_{mp,\omega})$).

III. Three-Phase Optimal Power Flow

The TOPF problem is formulated from current injections [27]. In the problem, the active power supplied by the PV plants is not controllable. However, these power plants can generate or absorb reactive power since the inverters can operate with power factors (PF) less than 1.

A. Modeling of PV Plant in the TOPF

The three-phase PV power plants are connected to the grid via a transformer. Depending on the capacity of the PV plant, the connection can be done without a transformer. In this study, the single-phase PVs are connected in the grid without transformer. The AC power supplied by the PV plant is:

$$P_{PV,\omega} = P_{PV,inv,\omega} N_{inv} \quad (9)$$

where N_{inv} the number of inverters.

If the PV plant operates with adjustable power factor within the inverter limits, its reactive generation, $Q_{PV,\omega}$ must respect the nominal inverter capacity, $S_{inv}^{\max}$, and its power factor, PF_{inv}, according to (10):

$$|Q_{PV}| \le \min\left\{\sqrt{\left(\frac{P_{PV,\omega}}{PF_{inv}}\right)^2 - \left(P_{PV,\omega}\right)^2},\ \sqrt{\left(S_{inv}^{\max} \times N_{inv}\right)^2 - \left(P_{PV,\omega}\right)^2}\right\} \quad (10)$$

B. TOPF Problem Formulation and Its Resolution

1) Objective Function

The performance index studied is the minimum voltage unbalance for all buses of the system, defined by their negative sequence component.

$$F = \min \sum_{k=1}^{n}\left(V_{\mathrm{Re},k,-}^2 + V_{\mathrm{Im},k-}^2\right) \quad (11)$$

where,

$$V_{k,-} = V_k^a + a^2 V_k^b + a V_k^c, \quad a = 1\angle 120°$$
$$V_k^{abc} = V_{\mathrm{Re},k}^{abc} + jV_{\mathrm{Im},k}^{abc}$$

V_k^{abc} is the three-phase voltage phasor of the bus k and the subscripts "Re" and "Im" indicate the real and imaginary part of the phasor.

2) Equality Constraints

The current balance in a given bus *k* of the system is made by adding the current injections per phase of the elements connected to this bus:

$$I_{g,k}^{abc} - I_{d,k}^{abc} - I_{k}^{abc} = 0 \tag{12}$$

where $I_{g,k}^{abc}$ are the contributions of generators, $I_{d,k}^{abc}$ the contributions of loads and I_{k}^{abc} the lines and transformers contributions connected to the phases *a*, *b* and *c* of the bus *k*.

Separating the real and imaginary parts of (12), the current balance equations of the TOPF are obtained:

$$\begin{aligned} I_{\mathrm{Re},g,k}^{abc} - I_{\mathrm{Re},d,k}^{abc} - I_{\mathrm{Re},k}^{abc} &= 0 \\ I_{\mathrm{Im},g,k}^{abc} - I_{\mathrm{Im},d,k}^{abc} - I_{\mathrm{Im},k}^{abc} &= 0 \end{aligned} \tag{13}$$

The currents injected by the generators are expressed by:

$$I_{g,k}^{abc} = I_{\mathrm{Re},g,k}^{abc} + jI_{\mathrm{Im},g,k}^{abc} = \left(\frac{P_{g,k}^{abc} + jQ_{g,k}^{abc}}{V_{k}^{abc}} \right)^{*} \tag{14}$$

where $P_{g_k}^{abc} and\ Q_{g_k}^{abc}$ are active and reactive powers generated. On the other hand, the currents consumed by the loads are:

$$I_{d,k}^{abc} = I_{\mathrm{Re},d,k}^{abc} + jI_{\mathrm{Im},d,k}^{abc} = \left(\frac{P_{d,k}^{abc} + jQ_{d,k}^{abc}}{V_{k}^{abc}} \right)^{*} \tag{15}$$

where $P_{d_k}^{abc}$ and $Q_{d_k}^{abc}$ are active and reactive powers consumed.

The current contributions of the lines are calculated by the network equations, expressed in matrix form as:

$$\begin{bmatrix} I_{\mathrm{Re},k}^{abc} \\ I_{\mathrm{Im},k}^{abc} \\ \vdots \\ I_{\mathrm{Re},m} \\ I_{\mathrm{Im},m}^{abc} \end{bmatrix} = \begin{bmatrix} G^{abc} & -\left(B^{abc}\right)^{t} & \cdots & -G^{abc} & B^{abc} \\ \left(B^{abc}\right)^{t} & G^{abc} & \cdots & -B^{abc} & -G^{abc} \\ \vdots & \vdots & \ddots & \vdots & \vdots \\ -G^{abc} & B^{abc} & \cdots & G^{abc} & -\left(B^{abc}\right)^{t} \\ -B^{abc} & -G^{abc} & \cdots & \left(B^{abc}\right)^{t} & G^{abc} \end{bmatrix} \cdot \begin{bmatrix} V_{\mathrm{Re},k}^{abc} \\ V_{\mathrm{Im},k}^{abc} \\ \vdots \\ V_{\mathrm{Re},m}^{abc} \\ V_{\mathrm{Im},m}^{abc} \end{bmatrix} \tag{16}$$

In (16), $G^{abc}\ and\ B^{abc}$ are 3×3 matrix composed of the real and imaginary parts of the elements of the admittance matrix of the system, $I_{\mathrm{Re},k}^{abc}, I_{\mathrm{Re},k}^{abc}, I_{\mathrm{Im},k}^{abc}$ and $I_{\mathrm{Im},m}^{abc}$ are vectors 3×1 and *t* indicates the transposed matrix.

The transformers and voltage regulators are considered fixed and represented by the π-equivalent circuit [39].

So that the voltages in the reference bus (*ref*) to be lagged of 120º, (17) is introduced into the formulation of the problem

$$\begin{aligned} V_{\mathrm{Im},ref}^{a} &= 0 \\ V_{\mathrm{Im},ref}^{b} - V_{\mathrm{Re},ref}^{b} \tan(-2\pi/3) &= 0 \\ V_{\mathrm{Im},ref}^{c} - V_{\mathrm{Re},ref}^{c} \tan(2\pi/3) &= 0 \end{aligned} \tag{17}$$

Finally, in order to keep the voltage magnitude of the reference bus equal in the three phases, (18) can be included in the TOPF model:

$$\begin{aligned} V_{\mathrm{Re},ref,a}^{2} + V_{\mathrm{Im},ref,a}^{2} - V_{\mathrm{Re},ref,b}^{2} - V_{\mathrm{Im},ref,b}^{2} &= 0 \\ V_{\mathrm{Re},ref,a}^{2} + V_{\mathrm{Im},ref,a}^{2} - V_{\mathrm{Re},ref,c}^{2} - V_{\mathrm{Im},ref,c}^{2} &= 0 \end{aligned} \tag{18}$$

3) Inequality Constraints

They represent operating limits and/or security aspects of the system. For each bus *k* and phases a, b and c, they are expressed by (19):

$$\begin{aligned} V_{\min,k}^{2abc} \le V_{\mathrm{Re},k}^{2abc} + V_{\mathrm{Im},k}^{2abc} \le V_{\max,k}^{2abc} \\ P_{g_{\min,k}}^{abc} \le P_{g,k}^{abc} \le P_{g_{\max,k}}^{abc} \\ Q_{g_{\min,k}}^{abc} \le Q_{g,k}^{abc} \le Q_{g_{\max,k}}^{abc} \end{aligned} \tag{19}$$

At the bus *k*, if there is a three-phase PV plant, in (19), $P_{g\min,k}^{abc} = P_{g\max,k}^{abc} = P_{PV,\omega}^{abc}$ and $Q_{g_k}^{abc} = Q_{PV,\omega}^{abc}$ with limits given in (10).

The TOPF problem was solved by the primal-dual interior point method [40].

IV. Results

The studies were performed with the IEEE34 bus system [41] in which the mutual impedances are not considered and the loads modeled as a constant power and a 70-bus system (SIS70) [42], a single-phase equivalent system transformed in a three-phase system by the addition of unbalance in the loads, maintaining the system's load in phase A and affecting the coefficients 0.8 and 0.6 respectively for the load in phase B and C. Solar irradiation and temperature data were obtained at the INMET station in Santa Marta – SC in January 2014. Data from the Hanwha SF220-30-1P240L (240Wp) panel and the SUNNY TRIPOWER 12000TL-US (12kVA, FP≥0.8) inverter are used. The barrier parameter and the tolerance adopted for all simulations were 10^{-10} and 10^{-6} respectively.

A. Output Power Generation of the Inverter

Fig. 3 shows the output power of the inverter on the day 23/01/2014, affected by the efficiency of the inverter, which varies from about 80% to about 97% depending on the irradiation and temperature. The maximum power point is achieved at 13 h.

B. Impact of PV Generation on the System

The PV plants were formed by connecting 48 SF220-30-1P240L panels per inverter, 24 of which were connected in series ($N_{PV,s} = 24$ and $N_{str} = 2$). The number of inverters was chosen according to the capacity of the plant. The single-phase PV has a capacity of 12kW and the three-phase PV a

capacity of 500 kW. One (01) three-phase PV connected to the bus 890 with 15 single-phase PVs were used for IEEE34 bus system and two (02) three-phase PVs connected to the buses 58 & 62 with 30 single-phase PVs for 70-bus system (SIS70). Single-Phase PV systems are distributed equally among the three phases of the system. These configurations have been adopted considering the loading of each system.

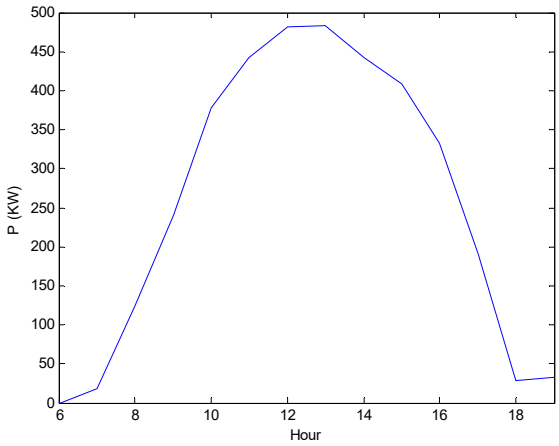

Fig. 3 Inverter Output Power on the day 23/01/2014

C.Simulation Results for a Specific Scenario of Irradiation and Temperature

The following results were obtained with PV systems operating at maximum power on the day 23/01/2014. Tables I and II indicate voltage unbalance and losses status for (i) operation mode without PV (base case), (ii) only three-phase PVs are allocated in the network with the unit power factor (PF=1) and (iii) single-phase and three-phase PVs operating with PF≠1. We can note in Table I that when single-phase and three-phase PV systems operate jointly with PF≠1, voltage unbalance level is considerably reduced. This operation mode contributes to improve the results presented in [37], wherein only three-phase PV systems were allocated. Table II shows the reduction in system losses when voltage unbalance is minimized.

TABLE I
IMPACT OF PV SYSTEMS ON VOLTAGE UNBALANCE

	Min. Unbal. (10^{-4})		
Systems	Base	PV/PF=1	PV/ PF≠1
IEEE34	2,98	3,33	1,81
SIS70	5,7	6,83	4,66

TABLE II
IMPACT OF PV SYSTEMS ON LOSSES

	Losses (kW)		
Systems	Base	PV/PF=1	PV/ PF≠1
IEEE34	100,74	52,24	46,04
SIS70	38,11	22,66	16,48

Figs. 4 and 5 present voltage profile for (i) only three-phase PV systems operating with PF=1, (ii) only three-phase PV systems operating with PF≠1 and (iii) association of single-phase and three-phase PV systems operating with PF≠1. The simulation results show that when the reactive power control of single-phase and three-phase PV systems association is taken into account, voltage profile almost coincides with its nominal value.

TABLE III
ACTIVE AND REACTIVE POWER INJECTIONS, IEEE34

	Active Power (kW) and Reactive Power (kVar)					
Without PV	Pg_{refa}	Pg_{refb}	Pg_{refc}	Qg_{refa}	Qg_{refb}	Qg_{refc}
	640,07	615,82	613,85	138,47	123,11	124,83
PV/PF=1	Pg_{refa}	Pg_{refb}	Pg_{refc}	Qg_{refa}	Qg_{refb}	Qg_{refc}
	493,58	468,13	465,28	131,54	115,14	117,18
	P_{PVa}	P_{PVb}	P_{PVc}	Q_{PVa}	Q_{PVb}	Q_{PVc}
	161	161	161	-	-	-
PV/PF≠1	Pg_{refa}	Pg_{refb}	Pg_{refc}	Qg_{refa}	Qg_{refb}	Qg_{refc}
	406,05	382,8	378,5	154	135,82	150,56
	P_{PVa}	P_{PVb}	P_{PVc}	Q_{PVa}	Q_{PVb}	Q_{PVc}
	161	161	161	-39,5	-39,5	-39,5

TABLE IV
ACTIVE AND REACTIVE POWER INJECTIONS, SIS70

	Active Power (kW) and Reactive Power (kVar)					
Without PV	Pg_{refa}	Pg_{refb}	Pg_{refc}	Qg_{refa}	Qg_{refb}	Qg_{refc}
	1127	898,5	671,5	889,62	710,31	531,70
PV/PF=1	Pg_{refa}	Pg_{refb}	Pg_{refc}	Qg_{refa}	Qg_{refb}	Qg_{refc}
	853,51	615,63	379,45	930,75	743,34	556,68
	P_{PVa}	P_{PVb}	P_{PVc}	Q_{PVa}	Q_{PVb}	Q_{PVc}
	161	161	161	-	-	-
PV/PF≠1	Pg_{refa}	Pg_{refb}	Pg_{refc}	Qg_{refa}	Qg_{refb}	Qg_{refc}
	684,88	459,01	235,89	847,21	652,30	511,28
	P_{PVa}	P_{PVb}	P_{PVc}	Q_{PVa}	Q_{PVb}	Q_{PVc}
	161	161	161	-3,22	-3,22	-3,22
	161	161	161	22,07	22,07	22,07

Tables III and IV show the active and reactive powers provided by the substation and the three-phase PV plants. Active power provided by the substation decreases with PV system operating. Depending on the grid utility, reactive power can be generated or absorbed when PV systems operate with PF≠1. Fig. 6 shows the reactive power provided by the substation for different operation modes of PV systems and Fig. 7, the contribution in the reactive power control of single-phase PVs, for IEEE34 feeder test. Note that the reactive power provided by the substation increases when PV systems operate with PF≠1. This result can be justified by the fact that the PV systems absorb more reactive power in the grid due to a very high current in the circuit. Also, this network consists of a very long and slightly charged feeder, which could lead to strong degradation of the voltage level. Table III shows reactive power absorbed by the three-phase PV plant and Fig. 7 shows that the single-phase PVs can generate or absorb reactive power depending on their location in the network. On the other hand, Fig. 8 shows that the reactive power injected by the PV power plants into the network has like consequence the reduction of the reactive power injected in the substation bus. This can be observed through Fig. 9, where there is a strong contribution of the reactive power injected by the single-phase PV plants, which contributes significantly in reducing the voltage unbalance and therefore losses as well.

Table IV also shows a distinct participation in the reactive power control of three-phase PVs for the 70-bus system.

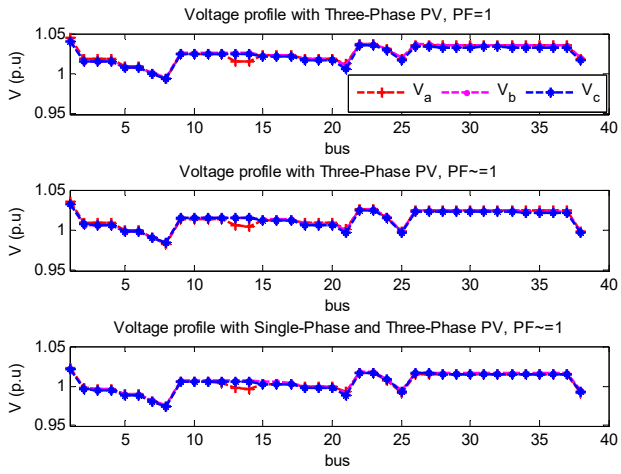

Fig. 4 Voltage profile, IEEE34

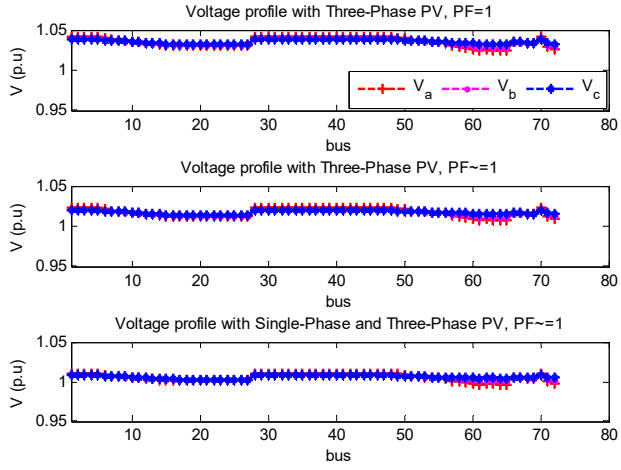

Fig. 5 Voltage profile, SIS70

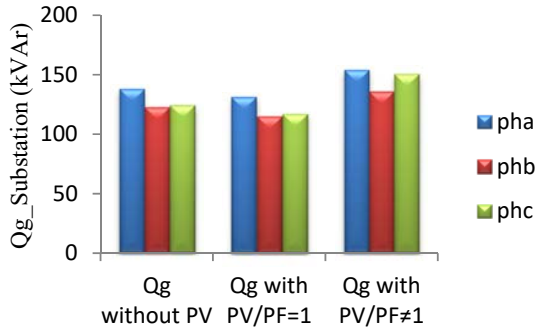

Fig. 6 Reactive power injection in the substation bus, IEEE34

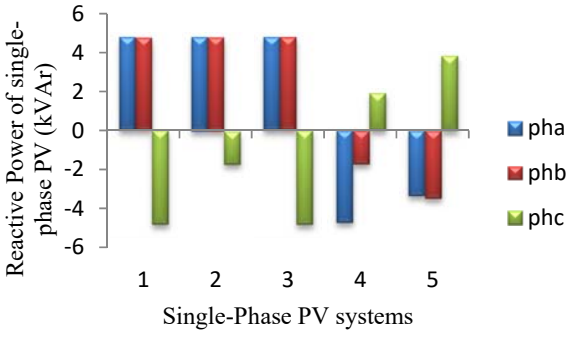

Fig. 7 Reactive power injection of single-phase PVs, IEEE34

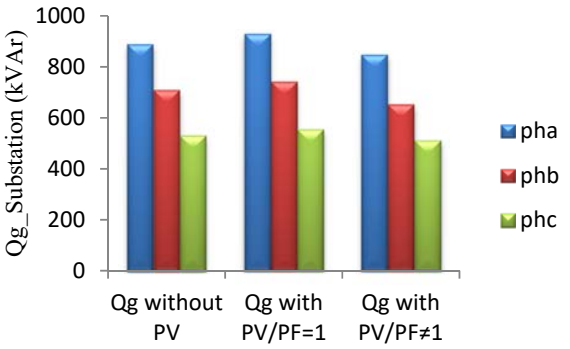

Fig. 8 Reactive power injection in the substation bus, SIS70

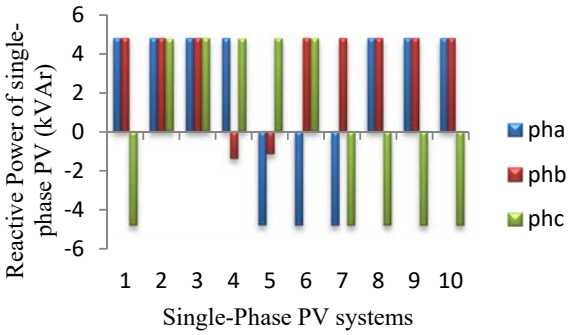

Fig. 9 Reactive power injection of single-phase PVs, SIS70

To better understand the impact of distributed allocation of PV systems on the voltage unbalance, we consider only the single-phase PVs allocated to the distribution systems studied, operating with unit power factor or with PF≠1. Figs. 10 and 11 show that when the single-phase PVs provide the grid with the reactive power, voltage profile becomes closer to the nominal. This aspect confirms the importance of distributed applications of PV systems and their contribution on the reduction of voltage unbalance when these are well located in the network.

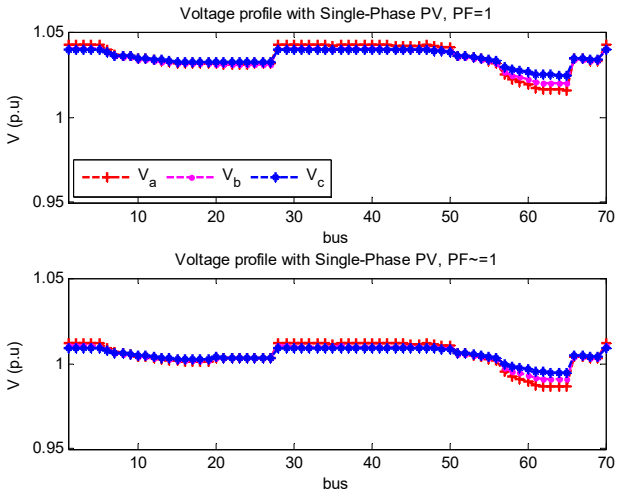

Fig. 10 Voltage profile with only single-phase PVs, SIS70

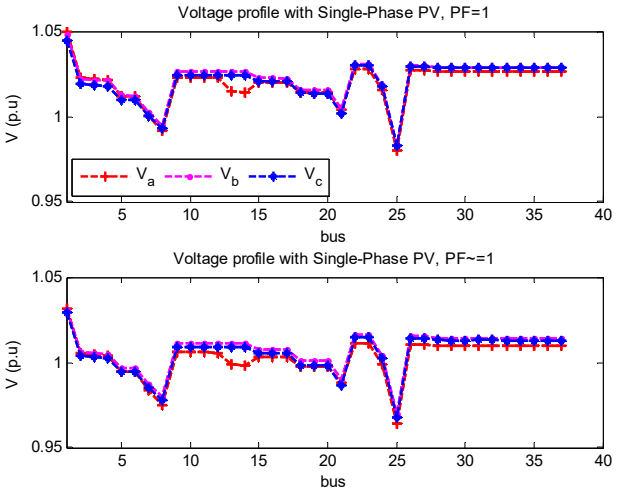

Fig. 11 Voltage profile with only single-phase PVs, IEEE34

V. Conclusion

In this paper, a tool for the analysis and simulation of unbalanced electrical networks was presented. The proposed tool took into account the modeling of single-phase and three-phase PV systems and used the primal-dual interior point method as an optimization technique for electrical networks. Compared to the results obtained in the previous research and taking into account the single-phase PV systems distributed between the phases of the grid, the OPF model has had a very significant effect in reducing the voltage unbalance and the losses in the distribution networks. The approach used for the positioning of single-phase PV installations in the network was based on the selection of the load buses, whereas for the three-phase PV systems, the choice was randomly made. This approach could affect the simulation results if the position of the PV plants is changed in the network. The use of a robust algorithm for optimal allocation of PV systems with other DG sources is currently under investigation.

Appendix

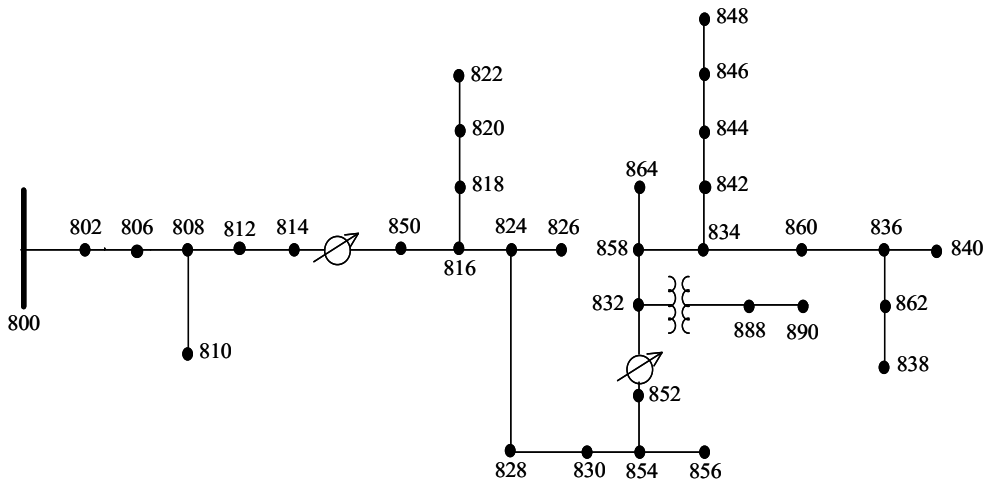

Fig. 12 IEEE34-bus

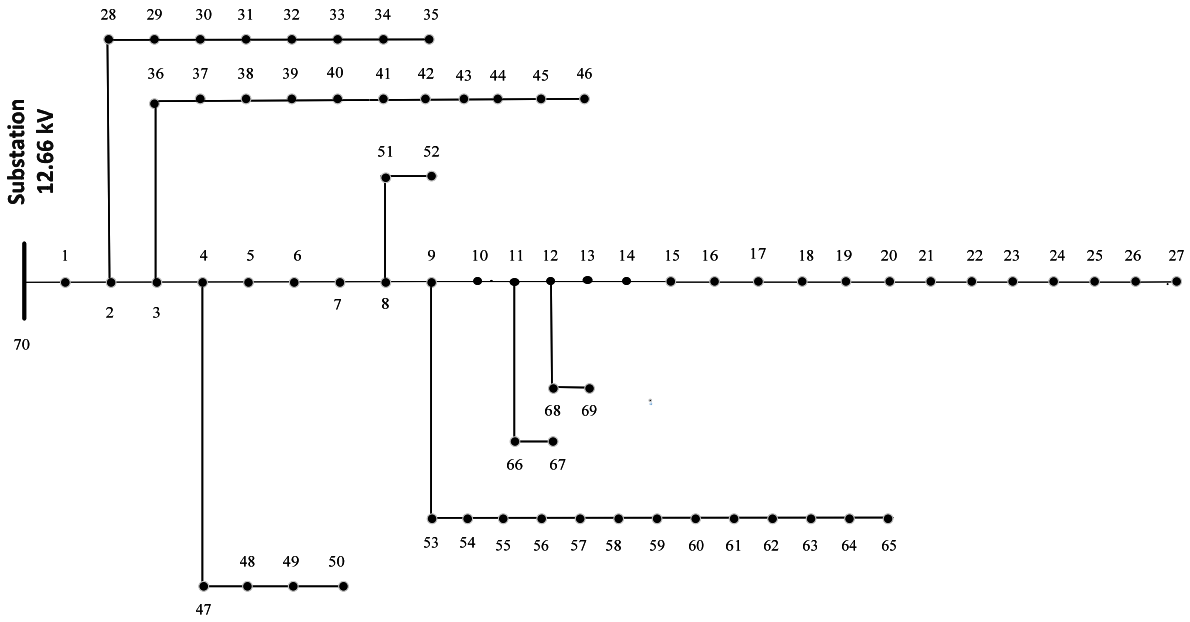

Fig. 13 SIS70-bus

ACKNOWLEDGMENT

This study is financially supported by the Conselho Nacional de Desenvolvimento Científico e Tecnológico (CNPq), Brazil.

REFERENCES

[1] S.P. Singh and A.R. Rao, "Optimal allocation of capacitors in distribution systems using particle swarm optimization," Electrical Power and Energy Systems/Elsevier, vol. 43, pp. 1267-1275, 2012.

[2] Qasim Kamil Mohsin, Xiangning Lin, Firas F.M. Flaih, Samir M. Dawoud, and Mohammed Kdair, "Optimal placement and capacity of capacitor bank in radial distribution system," in 2016 International Conference on Energy Efficient Technologies for Sustainability (ICEETS), 2016, pp. 416-423.

[3] Benemar Alencar de Souza and Angelo Márcio Formiga de Almeida, "Multiobjective Optimization and Fuzzy Logic Applied to Planning of the Volt/Var Problem in Distributions Systems," IEEE Transactions on Power Systems, vol. 25, no. 3, pp. 1274-1281, 2010.

[4] Yutian Liu, Peng Zhang, and Xizhao Qiu, "Optimal Reactive Power and Voltage Control for Radial Distribution System," in 2000 Power Engineering Society Summer Meeting (Cat. No.00CH37134), 2000, pp. 85-90.

[5] B. Mozafari, A.M. Ranjbar, A.R. Shirani, and A.Mozafari, "Reactive Power Management in a Deregulated Power System with Considering Voltage Stability: Particle Swarm Optimisation Approach," in CIRED 18th International Conference on Electricity Distribution, 2005.

[6] Sumit Paudyal, Claudio A. Cañizares, and Kankar Bhattacharya, "Optimal operation of distribution feeders in smart grids," IEEE Trans. on Industrial Electronics, vol. 58, no. 10, pp. 4495 - 4503, 2011.

[7] Antonio R. Baran and Thelma S.P. Fernandes, "A three-phase optimal power flow applied to the planning of unbalanced distribution networks," Electrical Power and Energy Systems, Elsevier, vol. 74, pp. 301-309, 2016.

[8] Nick C. Woolley and Jovica V. Milanovic, "Statistical Estimation of the Source and Level of Voltage Unbalance in Distribution Networks," IEEE Transactions on Power Delivery, vol. 27, no. 3, pp. 1450-1460, 2012.

[9] Ravindra Singh, Bikash C. Pal, and Richard B. Vinter, "Measurement Placement in Distribution System State Estimation," IEEE Transactions on Power Systems, vol. 24, no. 2, pp. 668-675, 2009.

[10] Philip P. Barker and Robert W. de Mello, "Determining the Impact of Distributed Generation on Power Systems: Part 1 - Radial Distribution Systems," in 2000 Power Engineering Society Summer Meeting (Cat. No.00CH37134), 2000, pp. 1645-1656.

[11] Carmen L. T. Borges and Djalma M. Falcão, "Optimal distributed generation allocation for reliability, losses, and voltage improvement," Electrical Power & Energy Systems. Elsevier, vol. 28, pp. 413-420, 2006.

[12] J. A. Peças Lopes, N. Hatziargyriou, J. Mutale, P. Djapic, and N. Jenkins, "Integrating distributed generation into electric power systems: A review of drivers, challenges and opportunities ," Electric Power Systems Research , vol. 77, pp. 1189-1203, 2007.

[13] Faruk Ugranl and Engin Karatepe, "Multiple-distributed generation planning under load uncertainty and different penetration levels," Electrical Power and Energy Systems, vol. 46, pp. 132-144, 2013.

[14] Mohammad Chehreghani Bozchalui, Chenrui Jin, and Ratnesh Sharma, "Rolling Stochastic Optimization based operation of distribution systems with PVs and Energy Storages," in Innovative Smart Grid Technologies Conference (ISGT), 2014 IEEE PES, 2014, pp. 1 - 5.

[15] E. Caamaño-Martín et al., "Interaction Between Photovoltaic Distributed Generation and Electricity Networks," Progress in Photovoltaics: Research and Applications Wiley InterScience, vol. 16, pp. 629-643, 2008.

[16] Mohamed A. Eltawil and Zhengming Zhao, "Grid-connected photovoltaic power systems: Technical and potential problems—A review," Renewable and Sustainable Energy Reviews/Elsevier, vol. 14, pp. 112-129, 2010.

[17] Farid Katiraei, Konrad Mauch, and Lisa Dignard-Bailey, "Integration of Photovoltaic Power Systems in High-penetration Clusters for Distribution Networks and Mini-Grid," International Journal of Distributed Energy Resources, vol. 3, no. 3, pp. 207-223, 2007.

[18] Davud Mostafa Tobnaghi, "A Review on Impacts of Grid-Connected PV System on Distribution Networks," International Jornal of Electrical, Computer, Energetic, Electronic and Communication Engineering, vol. 10, no. 1, pp. 137-142, 2016.

[19] Chao-Shun Chen, Chia-Hung Lin, Wei-Lin Hsieh, Cheng-Ting Hsu, and Te-Tien Ku, "Enhancement of PV Penetration With DSTATCOM in Taipower Distribution System," IEEE Transaction on Power Systems, vol. 28, no. 2, pp. 1560-1567, 2013.

[20] Shih-Chien Hsieh, "Economic Evaluation of the Hybrid Enhancing Scheme With DSTATCOM and Active Power Curtailment for PV Penetration in Taipower Distribution Systems," IEEE Transactions on Industry Applications, vol. 51, no. 3, pp. 1953-1961, 2015.

[21] Fabio L. Albuquerque, Adélio J. Moraces, Geraldo C. Guimarães, Sérgio M. R. Sanhueza, and Alexandre R. Vaz, "Photovoltaic solar system connected to the electric power grid operating as active power generator

and reactive power compensator," Solar Energy, Elsevier, vol. 84, pp. 1310-1317, 2010.
[22] Alessia Cagnano, Marco Liserre Enrico De Tuglie, and Rosa A. Mastromauro, "Online Optimal Reactive Power Control Strategy of PV Inverters," IEEE Transactions on Industrial Electronics, vol. 58, no. 10, pp. 4549-4558, 2010.
[23] M. J. E. Alam, K. M. Muttaqi, and D. Sutanto, "A Three-Phase Power Flow Approach for Integrated 3-Wire MV and 4-Wire Multigrounded LV Networks With Rooftop Solar PV ," IEEE Transactions on Power Systems, vol. 28, no. 2, pp. 1728-1737, 2013.
[24] A. von Jouanne and B. Banerjee, "Assessment of Voltage Unbalance," IEEE Transactions on Power Delivery, vol. 16, no. 4, pp. 782-790, 2001.
[25] Carol S. Cheng and Dariush Shirmohammadi, "A three-phase power flow method for real-time distribution system analysis," IEEE Trans. on Power System, vol. 10, no. 2, pp. 671-679, 1995.
[26] P. A. N. Garcia, J. L. R. Pereira, S. Carneiro, V. M. da Costa, and N. Martins, "Three-phase power flow calculations using the current injection method," IEEE Trans. on Power Systems, vol. 15, no. 2, pp. 508 - 514, 2000.
[27] L.R. Araujo, D. R. R. Penido, S. Carneiro, and J. L. R. Pereira, "A three-phase optimal power flow algorithm to mitigate voltage unbalance," IEEE Trans. on Power Delivery, vol. 28, no. 4, pp. 2394-2402, 2013.
[28] Sergio Bruno, Silvia Lamonaca, Ugo Stecchi, and Massimo La Scala, "Unbalanced three-phase optimal power flow for smart grids," IEEE Trans. on Industrial Electronics, vol. 58, no. 10, pp. 4504-4513, 2011.
[29] Emiliano Dall'Anese, Hao Zhu, and Georgios B. Giannakis, "Distributed optimal power flow for smart microgrids," IEEE Trans. on Smart Grid, vol. 4, no. 3, pp. 1464-1475, 2013.
[30] Leandro Ramos de Araujo, Débora Rosana Ribeiro Penido, and Felipe de Alcântara Vieira, "A multiphase optimal power flow algorithm for unbalanced distribution systems," Electrical Power and Energy Systems, Elsevier, vol. 53, pp. 632-642, 2013.
[31] Jie Wei, Leslie Corson, and Anurag K Srivastava, "Three-Phase Optimal Power Flow Based Distribution Locational Marginal Pricing and Associated Price Stability," in 2015 IEEE Power & Energy Society General Meeting, 2015, pp. 1-5.
[32] Yann Riffonneau, Seddik Bacha, Franck Barruel, and Stephane Ploix, "Optimal Power Flow Management for Grid Connected PV Systems with Batteries," IEEE Transactions on Sustainable Energy, vol. 2, no. 3, pp. 309-320, 2011.
[33] W. De Soto, S.A. Klein, and W.A. Beckman, "Improvement and validation of a model for photovoltaic array performance," Solar Energy, Elsevier, vol. 80, pp. 78-88, 2006.
[34] Marcelo Gradella Villalva, Jonas Rafael Gazoli, and Ernesto Ruppert Filho, "Comprehensive approach to modeling and simulation of photovoltaic arrays," IEEE Trans. on Power Electronics, pp. 1198-1208, 2009.
[35] Wang Yi-Bo, Wu Cuhn-Sheng, Liao Hua, and Xu Hong-Hua, "Steady-state model and power flow analysis of grid connected photovoltaic power system," in IEEE International Conference on Industrial Technology, Chengdu, 2008, pp. 1-6.
[36] Junior Edemilson Luiz Rangel, "Modelagem de Centrais Fotovoltaicas no Problema de Fluxo de Potência ótimo," Universidade Federal de Santa Catarina, 2015.
[37] Malinwo E. Ayikpa, Katia C. Almeida, and Guilherme C. Danielski, "Three-Phase Optimal Power Flow for Study of PV Plant Distributed Impact on Distribution Systems ," David Publishing Journal of Electrical Engineering , pp. 47-56, 2017.
[38] Huan-Liang Tsai, Ci-Siang Tu, and Yi-Jie Su, "Development of Generalized Photovoltaic Model Using MATLAB/Simulink," in World Congress on Engineering and Computer Science, San Francisco USA, 2008.
[39] Alcir José Monticelli, Fluxo de Carga em Redes de Energia Elétrica: Edgard Blücher Ltda, 1983.
[40] S.-C Fang and S. Puthempura, Linear Optimization and Extensions: Prentice-Hall, 2003.
[41] IEEE Test Feeders. (2013, April) IEEE Test Feeders. (Online). Available: http://ewh.ieee.org/soc/ (Accessed on 04/2016.)
[42] Hsiao-Dong Chiang and Renk Jean-Jumeau, "Optimal Network Reconfigurations in Distribution Systems: Part 2: Solution Algorithms and Numerical Results," IEEE Transactions on Power Delivery, vol. 5, no. 3, pp. 1568-1574, 1990.